

对高斯投影分带的研究

胡圣武

(河南理工大学 测绘学院, 河南 焦作 454000)



摘要: 对目前高斯投影分带理论中高斯投影分带的区域性、高斯投影带号的理解、高斯投影横坐标的认识和高斯投影带之间坐标的转换等问题进行了研究; 对产生这些问题的原因进行了分析, 并初步找到了解决问题的方法。

关键词: 高斯投影; 分带; 区域性; 转换

中图分类号: P226.1

文献标志码: B

文章编号: 1672-4623 (2012) 01-0054-03

我国在 20 世纪 50 年代规定大于和等于 1 : 500 000 的地形图采用的高斯投影^[1]。根据对地图精度的要求, 我国规定比例尺大于和等于 1 : 10 000 地图采用 3° 带投影, 比例尺小于和等于 1 : 25 000 地图采用 6° 带投影^[2-3]。因此对高斯投影分带研究是非常有意义和必要的, 本文就对目前高斯投影分带认识上存在的问题进行了研究。

1 投影分带的基本理论

高斯投影是一种横轴等角切圆柱投影, 为了控制投影变形不致过大, 保证地形图精度, 高斯投影通常采用分带投影方法。按一定经差将地球椭球面划分成若干投影带, 这是高斯投影中限制长度变形最有效的方法。分带时既要控制长度变形使其不大于测图误差, 又要使带数不致过多以减少换带计算工作。

目前高斯投影分带主要是 3° 带投影和 6° 带投影, 划分带号方法如图 1 所示。

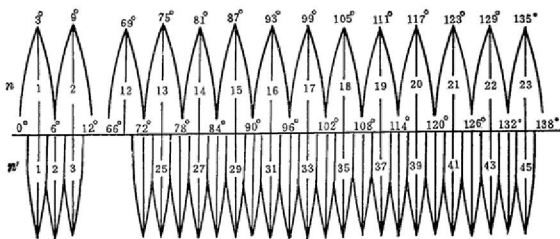


图 1 高斯投影分带示意图

高斯投影分带后, 各带分别投影, 各自建立坐标网, 如图 2 所示。

1.1 6° 分带法

6° 分带投影是从零子午线起, 由西向东, 每 6° 为一带, 全球共分为 60 带, 用阿拉伯数字 1、2、...、60 标记, 凡是 6° 的整数倍的经线皆为分带子午线, 见图 1。每带的中央经线度数 L_0 和代号 n 用式 (1) 求出:

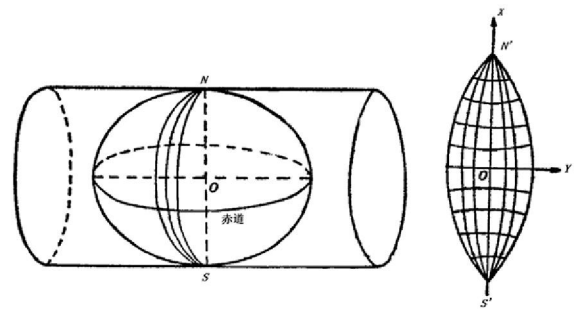


图 2 高斯投影与坐标轴示意图

$$L_0 = 6^\circ \cdot n - 3^\circ$$
$$n = \left[\frac{L}{6^\circ} \right] + 1 \quad (1)$$

式中, $[]$ 表示商取整; L 为某地点的经度。

1.2 3° 分带法

从东经 1° 30' 起算, 每 3° 为一个投影带, 将全球分为 120 带, 用阿拉伯数字 1、2、...、120 标记, 见图 1。这样分带的目的在于使 6° 带的中央经线全部为 3° 带的中央经线, 即 3° 带中有半数的中央经线同 6° 带的中央经线重合, 以便在由 3° 带转换为 6° 带时, 不需任何计算, 而直接转用。每带的中央经线度数 L_0 和代号 n 用式 (2) 求出:

$$L_0 = 3^\circ \cdot n$$
$$n = \left[\frac{L + 1^\circ 30'}{3^\circ} \right] \quad (2)$$

式中, $[]$ 表示商取整; L 为某地点的经度。

2 高斯投影分带的带号

由于我国的陆地主要分布在精度 72° ~ 136° 之间。我国横跨 11 个 6° 带和 22 个 3° 带, 根据公式 (1) 和 (2) 可以计算出我国主要陆地所在的带号范围: 6° 带: 13 ~ 23; 3° 带: 24 ~ 45。

因此我国 3° 带与 6° 带之间没有重号出现, 这也

收稿日期: 2011-07-13

项目来源: 国家自然科学基金资助项目 (40474003)。

意味着我国的高斯坐标都是唯一的,不可能 1 个点既是 3°带坐标又是 6°带坐标,只能要么是 3°带坐标要么是 6°带坐标。如坐标 $x=1\ 026\ \text{km}$, $y=25\ 452.678\ \text{km}$, 这个点的带号是 25,所以说只能是 3°带的坐标,而不可能是 6°带的坐标。

3 投影分带的地域性

有关高斯投影分带的地域性主要表现在 2 个方面。

1)高斯投影并不是在世界都采用,目前只在我国、蒙古、朝鲜等国家使用。美国陆地就不采用高斯投影,而是通用横轴墨卡托投影(Universal Transverse Mercator Projection)取前面 3 个英文字母大写而称 UTM 投影。它与高斯-克吕格投影相比较,这 2 种投影之间仅存在 2 点区别^[2-4]:高斯投影中央经线长度比为 1,而 UTM 投影的中央经线长度比为 0.9996;划带的方法不同。关于高斯-克吕格投影带的划分,它的分带是从零子午线向东 6°为一带;通用横轴墨卡托投影的分带是从 180°起向东每 6°为一带,即与国际百万分之一地图的划分一致,也就是高斯-克吕格投影的第 1 带(0°~6°E)为 UTM 投影的第 31 带;UTM 的第 1 带(180°~174°W)是高斯-克吕格投影的 31 带。

2)目前我们所采用的高斯投影主要是指在我们国家范围之内,其高斯坐标范围也是在我国范围内,超过我国范围就不予研究。对于这一点的认识与理解还存在着很多问题。把高斯投影坐标看作是纯数学问题。如这样的坐标: $x=5\ 060\ 000\ \text{m}$, $y=9\ 307\ 000\ \text{m}$ 。按高斯投影理论,这个点在第 9 投影带;而我国的 6°带在 13~23,3°带在 24~45。因此该点坐标不在我们国家,因此从数学上看这样的坐标是存在的,而从实际意义来说此点不存在,不应该有这样的坐标。

4 高斯投影的 y 坐标

高斯投影为了区分每带的坐标,通常的成果形势是通用坐标值,而不是自然坐标值。一般而言 x 坐标不动,主要是对 y 坐标值进行处理,主要是对 y 坐标值加上 500 km,然后在前面加上两位数的带号。

下面先来解释对 y 坐标加 500 km 的理由:对于 6°带而言,所跨纬度为 6°,以赤道为 y 坐标,则横坐标的所跨长度为 D:

$$D = R * \pi * 6^\circ \div 180^\circ$$

以 $R=6\ 400\ \text{km}$ 代入,则得:

$$D \approx 6400 * \pi * 6^\circ \div 180^\circ$$

$$\approx 670\ \text{km}$$

$$\text{则: } -350\ \text{km} \leq y \leq 350\ \text{km}$$

要使 y 坐标为正,实际上只要加上 400 km,而实际上采用的是加上 500 km。对 y 坐标加上一个值实际上有 2 个目的:使 y 坐标值都为正;使 y 坐标具有相同的坐标位数。因此,加上 400 km 不能满足第 2 个条件;而对 y 坐标加上 500 km 后就满足了 2 个条件,为了计算方面,就取 500 km。

5 高斯投影带坐标之间的转换

高斯投影带之间坐标转换是在同一个椭球体上条件下进行的。

高斯投影坐标之间的转换主要分为 2 种情况:3°带向 6°带的转换;6°带向 3°带的转换,我们就这两种情况加以研究。

5.1 3°带向 6°带的坐标转换

3°带向 6°带坐标转换可以分为 2 种类型:同中央经线转换和不同中央经线转换。

1)同中央经线。如果 2 个点的坐标的中央经线是相同,则转换坐标比较简单,方法如下:首先 x 坐标不变,然后把 y 坐标去掉旧的带号换成新的带号即可。

$$\text{如: } A: x=1015\ 125.678\ \text{m}, y=27\ 710\ 234.787\ \text{m}$$

$$B: x=1034\ 256.125\ \text{m}, y=14\ 821\ 563.128\ \text{m}$$

现在要把 A 点坐标转换到 B 的投影带上。A 点带号为 27,因此在 3°带,其中央经线 L_A , B 点带号为 14,因此在 6°带上,其中央经线 L_B ,由公式(1)和

(2) 计算得:

$$L_A = 27 * 3^\circ = 81^\circ$$

$$L_B = 14 * 6^\circ - 3^\circ = 81^\circ$$

因此两点的中央经线一致。

A 点坐标转换到 B 的投影带坐标为:

$$x=1\ 015\ 125.678\ \text{m}, y=14\ 710\ 234.787\ \text{m}$$

2)不同中央经线。如果 2 个点的坐标的中央经线不同,则坐标转换方法如下:

首先,用高斯反算公式计算要转换点大地坐标的(B, L),见式(3)。

$$B = B_l - \frac{t_l}{2M_l N_l} y^2 + \frac{t_l}{24M_l N_l^3} (5 + 3t_l^2 + \eta_l^2 - 9\eta_l^2 t_l^2) y^4 - \frac{t_l}{720M_l N_l^5} (61 + 90t_l^2 + 45t_l^4) y^6 \tag{3}$$

$$l = \frac{1}{N_l \cos B_l} y - \frac{1}{6N_l^3 \cos B_l} (1 + 2t_l^2 + \eta_l^2) y^3 +$$

$$\frac{1}{120N_l^5 \cos B_l} (5 + 28t_l^2 + 24t_l^4) y^5$$

$$\text{则要转换点的大地坐标为: } \begin{matrix} B = B \\ L = L_0 + l \end{matrix}$$

再计算所要转换到投影带的中央经线 L_6 ; 然后计算 ΔL : $\Delta L = L - L_6$; 再把 $(B, \Delta L)$ 代入高斯正算公式 (4), 其中 l 用 ΔL 代入, 并化成弧度, 计算坐标 (x, y) 。

$$x = s + \frac{l^{n^2} N}{2\rho^{n^2}} \sin \varphi \cos \varphi + \frac{l^{n^4} N}{24\rho^{n^4}} \sin \varphi \cos^3 \varphi$$

$$(5 - \tan^2 \varphi + 9\eta^2 + 4\eta^4) + \dots$$

$$y = \frac{l^n N \cos \varphi}{\rho} + \frac{l^3 N}{6\rho^3} \cos^3 \varphi (1 - \tan^2 \varphi + \eta^2) +$$

$$\frac{l^5 N}{120\rho^5} \cos^5 \varphi (5 - 18 \tan^2 \varphi + \tan^4 \varphi) + \dots$$
(4)

最后, 把计算的 (x, y) 转换为通用坐标即为所求。

5.2 6°带坐标转换 3°带坐标

6°带坐标转换 3°带坐标也分 2 种类型即同中央经线与不同中央经线。

1) 同中央经线。如果 2 个点的坐标的中央经线是相同, 则转换坐标比较简单, 方法如下: 首先坐标不变; 然后把坐标去掉旧的带号换成新的带号即可。

如: $A: x = 1034256.125m, y = 14821563.128m$

$B: x = 1015125.678m, y = 27710234.787m$

现在要把 A 点坐标转换到 B 的投影带上。A 点带号为 14, 因此在 3°带, 其中央经线 L_A , B 点带号为 27, 因此在 6°带上, 其中央经线 L_B , 由公式 (1) 和 (2) 计算得:

$$L_A = 14 \times 6^\circ - 3^\circ = 81^\circ$$

$$L_B = 27 \times 3^\circ = 81^\circ$$

因此两点的中央经线一致。

A 点坐标转换到 B 的投影带坐标为:

$$x = 1034256.125m, y = 27821563.128m$$

2) 不同中央经线。6°带坐标转换为 3°带坐标, 其方法如下:

计算 6°带坐标的大地坐标 (B, L) , 用公式 (3);

计算要转换到 3°带坐标的中央经线的经度;

计算 ΔL , $\Delta L = L - L_3$;

把 $(B, \Delta L)$ 代入公式 (4), 计算 (x, y) ;

把 (x, y) 转换为通用坐标, 即为所求结果。

6 结 语

本文对高斯投影的几个基本问题进行了研究, 不过高斯投影所要研究的问题还很多, 如高斯投影分带坐标转换的精度问题^[5-6], 分带大小如何满足目前高精度工程精度需要等问题亟需研究^[7]。

参考文献

[1] 孙达, 蒲英霞. 地图投影[M]. 南京: 南京大学出版社, 2005

[2] 胡圣武. 地图学[M]. 北京: 清华大学出版社, 2008

[3] 祝国瑞. 地图学[M]. 武汉: 武汉大学出版社, 2004

[4] 高井祥. 测量学[M]. 北京: 中国矿业大学出版社, 2004

[5] 王煥改, 马朝旭, 贾文景, 等. 60 带和 30 带图形的叠加[J]. 物探装备, 2006, 12(4): 303-305

[6] 赵俊生, 刘雁春, 王克平, 等. 关于高斯投影长度变形的探讨[J]. 海洋测绘, 2007, 27(3): 9-11

[7] 梅熙. 高斯投影变形对高速铁路线路设计的影响[J]. 铁道工程学报, 2010, 10: 52-57

作者简介: 胡圣武, 博士, 副教授, 现主要从事 GIS 基础理论和图像处理技术研究。

(上接第 53 页)

北京: 科学出版社, 2010

[3] 范志全, 范平, 张少白, 等. 一种无失真图像数据压缩算法[J]. 计算机应用, 2001, 21(8): 134-137

[4] 商进, 张礼勇. 一种双游程编码的测试数据压缩方案[J]. 哈尔滨理工大学学报, 2010, 15(4): 19-22

[5] 刘於勋, 李国伟, 马丽. 浅谈栅格数据结构及其压缩编码方法[J]. 郑州工业高等专科学校学报, 2001, 20(3): 5-12

[6] Gregory A Plumb. Compression of Continuous Spatial Data in the Raster Digital Format[J]. Computers & Geosciences, 1993, 19 (4): 493-497

[7] David A Huffman. A Method for the Construction of Minimum-Redundancy Codes [J]. Proceedings of the IRE, 1952 (9): 1098-1101

第一作者简介: 闵轩, 硕士, 主要研究地理信息系统。

geological data, which organically integrated together the geological attribute data, geospatial data and geological maps in the geographical position. It had been proved that open spacial database could manage ,communicate, analyze, extract, and update the geological information effectively, and had great important auxiliary function in paleogeographic study. With the increasing geological data, the paleogeography maps would become more accurate gradually by the improving of the applicability, efficiency and intuitiveness.

Key words open spatial database , ArcGIS , paleogeography
(Page:29)

Study on Remote Sensing Image Classification Based on Texture and BP Neural Network by XIA Haoming

Abstract In the methods of improving the classification precision of remote sensing images, adding textural information as an expanded eigenvector into feature space is a pretty useful method. In this paper, the author extracted texture using spatial connections between geo-objects, then put it into the BP network classification process. This experiment showed a nice result.

Key words texture , gray level cooccurrence matrix , BP network , Remote Sensing Image , filtering
(Page:33)

Obtain Method of the Coastal Zone Topographic Map Based on LIDAR Technique by LIN Xianxiu

Abstract In recent years, as a new active remote sensing technique, airborne LIDAR system made breakthrough progress in real time acquisition of the surface 3D space information . This paper briefly introduced the technology of Pingtan comprehensive experimental area topographic map acquisition by LIDAR.

Key words LIDAR , remote sensing , digital line graphic , research
(Page:37)

Research on Chongqing Urban Forest System Based on RS and GIS by XIONG Wenquan

Abstract Based on 0.5 m high resolution Geoeye satellite image, it analyzed Chongqing urban forest system sight structure style under Remote Sensing and GIS system, choosing some guideline such as diversity, predominance, uniformity and its stave. Finally, it concluded some advice on the establishment of city forest system.

Key words RS, GIS, city forest, sight structure style
(Page:39)

Key Technology of Generating 3D Scene in OSG by XIANG Jie

Abstract With the development of various 3D rendering engines based on OpenGL, the full use of these engines has become the most primary problem . OpenSceneGraph, rendering engine of one high performance, open source is also paid people' more attention. This article systematically analysed OSG structure and feature, studied construction process of 3D scene and some key technologies with OSG.

Key words OSG , 3D scene , rendering engine , subset , data organization , cutting , building technology , terrain generating
(Page:43)

Patterns Analysis and Practice of Building GIS on Existing Operation Management System by QIU Xiangfeng

Abstract With development of informationization , collaborative management has been used in more and more domain. The paper introduced basic concept of collaborate and collaborative management software, taking "Water Conservancy Management Information System of Xiamen City " as an example, analysed the application of collaborative management to water conservancy management domain, proposed a framework of water conservancy E-government construction and the concrete construction content.

Key words existing operations management system, GIS, building pattern
(Page:46)

Impacts on the Land Surface Temperature for Different Methods of Land Surface Emissivity Estimation by XIAO Yao

Abstract In these methods, land surface emissivity is the key parameter, so land surface emissivity estimation has a direct impact on the land surface temperature results. Now, NDVI is used for land surface emissivity retrieval frequently. In this paper, in order to get the land surface temperature of Beijing, the writer used Van's land surface emissivity estimation method and a combination of Qin Zhihao's and Sobrino's estimation methods, then compared the two results. The results showed that these two estimation methods were both suitable for farmland and forest land, but for water and urban, with the purpose of getting a more accurate land surface temperature results, comparing the local measured data and retrieval results , and then confirming the more appropriate estimation method.

Key words land surface emissivity , land surface temperature , Beijing
(Page:48)

Compression Method of Improved Block Coding by MIN Xuan

Abstract A compression method of improved block coding was introduced, and the implementation steps were given. Experiments had proved that the improved block coding has higher compression ratio and better adaptability feature than traditional one.

Key words improved block code , data compression , compression ratio
(Page:52)

Research on Gauss-Kruger Projection Division by HU Shengwu

Abstract The paper researched several problems that Gauss-Kruger projection theory exists at present. They were mainly Gauss-Kruger projection regionality, cognition of Gauss-Kruger projection dividing number, comprehension of Gauss-Kruger projection abscissas and axis transformation about Gauss-Kruger projection division. It analysed causes that these problems exist and solved these basic problems.

Key words Gauss-Kruger projection , dividing number , regionality , transformation
(Page:54)

Visibility Analysis of Battlefield Environment Based on Urban Building by WANG Mingxiao

Abstract This article proceeded from the reality of urban warfare, according building as main consideration to take visibility analysis. It proposed the method that made visibility analysis in urban battlefield environment with DEM stacking building height information, and researched the data types which should be selected in urban battlefield environment, analyzed the quick acquisition channels of getting DEM and building height information as well as the characteristic of each manner. It had took some experiment with different regions datas, such as Lanzhou, Urumchi, Xining , and also verified feasibility and accuracy of this method.

Key words visibility analysis , building height information , acquisition channels , TIN model , DEM
(Page:57)

Research on NDVI of Sewage Irrigation Area Based on HJ-1A-B Data by CHANG Fangyun

Abstract The study of Vegetation Index of sewage irrigation area has guiding significance to the sewage disposal, ecological protection and so on. This thesis, taking advantage of 21 CCD image data of the Chinese environmental and disaster monitoring and forecasting of small satellites (HJ-1A-B) during 2008-2010, selected sewage irrigation area and clean water irrigation area which is typical and easy to be compared. Then, every average NDVI was extracted from every area in those images over 3 years. Finally, those NDVI mean values were compared horizontally and longitudinally comparison. Experimental results show that, NDVI can monitor vegetation change in dynamically; the vegetation index's trends over time in both sewage irrigation area and clean